Metastability, adiabatic shear bands initiation and plastic strain localization in the AMg6 alloy under dynamic loading

Mikhail Sokovikov, Sergey Uvarov
Institute of Continuous Media Mechanics of the Ural Branch of the Russian Academy of Sciences, Russia
sokovikov@icmm.ru, http://orcid.org/0000-0003-0298-6240/
usv@icmm.ru, http://orcid.org/0000-0002-7538-0971/

Mikhail Simonov
Perm National Research Polytechnic University, Russia
elferok@gmail.com, http://orcid.org/0009-0002-7096-0966/

Vasiliy Chudinov, Oleg Naimark
Institute of Continuous Media Mechanics of the Ural Branch of the Russian Academy of Sciences, Russia
chudinov@icmm.ru, http://orcid.org/0000-0002-4109-1573/
naimark@icmm, http://orcid.org/0000-0001-6537-1177/

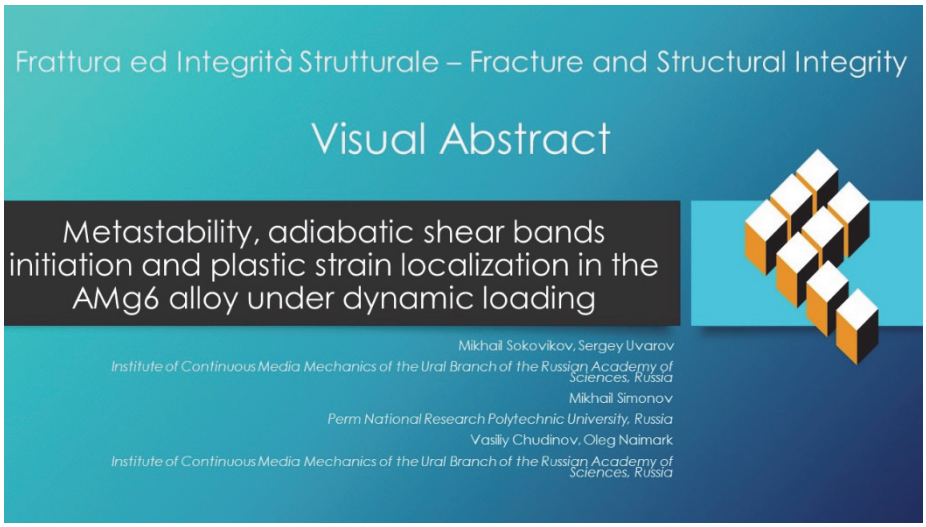

Citation: Sokovikov, M., Uvarov, S., Siimonov, M., Chudinov, V., Naimark, O., Metastability, adiabatic shear bands initiation and plastic strain localization in the AMg6 alloy under dynamic loading, Frattura ed Integrità Strutturale, 68 (2024) 255-266.

Received: 29.06.2023
Accepted: 05.02.2024
Published: 19.02.2024
Issue: 04.2024

KEYWORDS. Plastic shear localization, Dynamic loading, Numerical simulation, Evolution of the defect structure, Structural studies.

INTRODUCTION

The extremely localized deformation zones known as adiabatic shear bands (ASB) with a few micrometers wide occur in materials resulting in the dynamic failure in the shear bands [1].

Several applications of this phenomenon follow from the mechanisms of transformation of the intense plastic shear to failure that is characteristic for shock impact loading, ballistic penetration, fragmentation, machining, explosive forming, [2,3].

The ASB definition is related to high strain rates, when temperature rise can be qualified as adiabatic [4-10].

The pioneering experimental study by Marchand and Duffy [7] established a three stages of ASB failure, starting from a homogeneous strain state transforming into the inhomogeneous strain distribution with following narrowing as the precursor of failure. The dissipation and initial microstructure inhomogeneities including grain and phase boundaries are the key factors in the ASB formation and transition to failure.

Backman and Finnegan [11,12], Wei and Batra [13,14] attracted the attention that shear bands instability have triggered from a defects (microshears, microcracks) similar to second phase and damage evolution decreases the instability threshold strain. Both features are characteristic for metastable critical systems.

However, it is still open problem whether the thermoplastic instability leads to shear bands in the presence the initial inhomogeneity [2]. Clifton [15] and Bai [16] studied the influence of initial periodic nonuniformities under simple shearing deformation and established that this disturbances, simulating the initial imperfections, could timely increase or decay depending on the spatial wavelength. Wright [17,18] studied the ASB susceptibility for different materials depending on the initial defects distribution that could scale the adiabatic material response[19] and ASB formation can be changed dramatically [7]. Clifton and Molinari [15], [20-22], Wright [23] proposed a scaling laws for the critical nominal strain as a logarithmic relationship between a defect induced nonuniformity parameter and a scaled critical strain that correctly predict plastic strain localization.

Original dynamic recrystallization (DRX) conception of ASB initiation and failure was developed by Rittel et al. [24, 25] based on the transformation of the dynamic stored energy of cold work into ASB structures. Important aspect is that DRX is developed at the stage, when the adiabatic heating effects are not «master» mechanism and DRX results from the critical value of stored energy due to dynamic deformation.

Structural aspects of ASB initiation under high-strain rate loading was studied by the transmission electron microscopy (TEM) and electron backscatter diffraction (EBSD) methods [26, 27, 28, 29]. Grain refining close to the diameters 200 nm was found as athermal mechanism of recrystallization initiated by multiscale shear interaction and analyzed by Nesterenko, Meyers and Wright [30] as self-organization process. Grady and Kipp [3, 31] discussed the links of this self-organization in the shear ensemble behavior with universality of steady-wave fronts and corresponding shear band spacing occurring within the shock process zone [32].

Despite the long history and significance in applications there is no general view concerning the mechanisms linking the ASB phenomena, the onset of unstable flow, dynamic strain localization and ASB failure. The shear band initiation and the growth, the interaction between shear bands, and the influence of these phenomena on the material and kinematic properties are not well understood. This review and the study of collective properties of microshears ensemble allow us to link the shear banding during the plastic shear localization with specific non-linearity (metastability) of the stored (free) energy release and corresponding driving force for defects kinetics starting from some critical level of stored energy.

As it was shown by Naimark [33] the collective behavior of microshears is realized as specific type of critical phenomenon, the structural-scaling transition in the metastability area of out-of-equilibrium free energy of material with microshears ensemble. The metastability decomposition proceeds with the formation of area with pronounced microshears orientation, jump-like microshear induced strain localized on characteristic spatial scales. Self-similar solutions of evolution equation for microshears ensemble were established governing the scaling properties of shear bands and providing both ASB staging of plastic flow localization and transition to failure.

DEFECTS INDUCED METASTABILITY, SELF-SIMILAR SOLUTIONS AND SCALING OF ASB KINETICS.

Free energy metastability. Structural-scaling transitions. Collective properties of microshear ensembles.

Statistical theory of mesoscopic defects established specific type of critical phenomena in solid with microshears (microcracks), the structural-scaling transitions, and allowed us to propose the phenomenology of plastic strain instability and damage localization [33]. The key results of the statistical approach and developed phenomenology are the establishment of specific non-linearity of free (stored) energy release in the terms of two "order parameters" responsible

for the structure evolution: the defect induced strain p_{ik} and the structural scaling parameter $\delta = (R/r_0)^3$. The structural-scaling parameter describes the initial and current susceptibility of material structure to the defects growth and represents the ratio of the spacing between defects R and characteristic size of defects r_0. Statistically predicted non-equilibrium free energy F represents generalization of the Ginzburg-Landau expansion in terms of mentioned order parameters and in the case of simple shear $p = p_{xz}$ read

$$F = \frac{1}{2} A(\delta,\delta_*) p^2 - \frac{1}{4} Bp^4 - \frac{1}{6} C(\delta,\delta_c) p^6 - D\sigma p + \chi \left(\frac{\partial p}{\partial x}\right)^2 \quad (1)$$

where $\sigma = \sigma_{xz}$ is the shear stress, χ is the non-locality parameter, A, B, C, D are the material parameters, δ_* and δ_c are characteristic values of structural-scaling parameter (critical points). Critical points define the areas of characteristic free energy non-linearity on the defects growth in corresponding ranges of δ:. $\delta < \delta_c \approx 1$, $\delta_c < \delta < \delta_*$, $\delta > \delta_* \approx 1.3$.

Free energy form (1) represents multi-wall potential with qualitative different metastability in the ranges $\delta_c < \delta < \delta_*$ and $\delta < \delta_c \approx 1$

Free energy release kinetics allows the presentation of damage evolution equation and kinetics for structural-scaling parameter in the form

$$\frac{dp}{dt} = -\Gamma_p \left(A(\delta,\delta_*) p - Bp^3 + C(\delta,\delta_C) p^5 - D\sigma - \nabla_l \left(\chi \nabla_l p \right) \right) \quad (2)$$

$$\frac{d\delta}{dt} = -\Gamma_\delta \left(\frac{1}{2} \frac{\partial A}{\partial \delta} p^2 - \frac{1}{6} \frac{\partial C}{\partial \delta} p^6 \right) \quad (3)$$

where Γ_p, Γ_δ, A, B, C, D are the kinetic coefficients. As it follows from the solution of Eqn. (2) the transitions over the bifurcation points δ_c and δ_* result in sharp changes in the metastability types and collective modes of defects.

Collective modes of defects as mechanism of ASB initiation and failure

The types of transitions over the critical points are given by the group properties of Eqns. (2), (3) for different ranges of the structural-scaling parameter $\delta (\delta > \delta_*, \delta_c < \delta < \delta_*, \delta < \delta_c)$. This equation has in the area $\delta > \delta_*$ the eigen forms as spatial-periodic modes S_1 on the scales Λ with week microshear orientation determined mainly by the stress field σ. For $\delta \to \delta_*$ this solution undergoes qualitative changes due to the divergence of inner scale Λ: $\Lambda \approx -\ln(\delta - \delta_*)$ and is transformed into the finite amplitude "breathers" modes for $\delta \to \delta_*$ (in the area $\delta > \delta_*$) and the solitary wave modes $p(\zeta) = p(x - \mathrm{V}t)$. The solitary wave solution describes the microshears kinetics in the orientation metastability area. The wave amplitude p, wave front velocity V and the width of wave front L_S are determined by the parameters of non-equilibrium transition in the metastability area

$$p = 1/2(p_a - p_m)\left[1 - \tanh\left(\zeta L_S^{-1}\right)\right], \; L_S = 4/(p_a - p_m)(2\chi/A)^{1/2} \quad (4)$$

The velocity of wave fronts is $V = \chi A(p_a - p_m)/\Gamma_p^2$, where $(p_a - p_m)$ is the jump in the value of p in the metastability area. These solitary waves represent the image of strain localization zones with the front, where the orientation transition is realized. A transition through the bifurcation point is accompanied by the appearance of spatio-temporal structures of a qualitatively new type characterized by explosive accumulation of defects as $t \to t_c$ in the spectrum of spatial scales ("blow-up" dissipative structures) [33]. It is shown that the developed stage of kinetics of in the limit of characteristic times can be described by the self-similar solution in the form

$$p(x,t)=\varphi(t)\,f(\zeta),\zeta=x/L_c,\varphi(t)\sim(t-t_c)^{-m} \quad (5)$$

where m is the parameter related to the nonlinearity type of Eq.2 for $\delta\langle\delta_C,p\rangle p_C$; t_c is the characteristic temporal scale of self-similar solution (5).

Specific form of the function $f(\zeta)$ can be determined by solving the corresponding eigen value problem. The scale L_c, so-called fundamental length [35], has the meaning of a spatial period of the solution (2). This self-similar solution describes the kinetics of the collective mode of defects in the "blow-up" regime: $p(x,t)\to\infty$ for $t\to t_c$ on the spectrum of spatial scales $L_H=\mathrm{kL}_c, k=1,2,...K$. In this case the complex "blow-up" structures appear on the scales $L_H=\mathrm{kL}_c$, when the distance between simple structures will be close to L_c.

The free energy form (1), corresponding free energy release in the presence of metastability and the types of microshears collective modes allowed the formulation of scenario of ASB initiation and transition to ASB failure as the critical behavior, the structural-scaling transition in the microshear ensemble [36]. This transition includes the consequent generation of different collective modes of microshears (the solitary waves and blow-up dissipative structures consecuently) due to the qualitative change of free-energy metastabilty and free energy release. The master variable, the structural-scaling parameter, describes the collective properties of microshears interaction and scaling transition due to the generation of the microshear collective modes. The staging of ASB initiation and ASB failure can be interpreted in terms of critical behavior of microshear ensemble. The velocity and the wave front length follow to the "metastability gap" and depend in the case of steady shock on stress amplitude. The self-similar nature of the solution (4) allows the explanation of the Swegle-Grady power universality [37] of the steady shock wave and provides the links with ASB and steady shock wave dynamics. The transition to the blow-up microshears dynamics allows the explanation of the third stage corresponding to ASB failure due to intensive microshear interaction, anomalous free energy release and dissipation on the spectrum of spatial scales L_H. This transformation could explain specific features of ASB structure evolution as sub-grain formation associated by Rittel [24] as the DRX phase transformation. The DRX transformation zones can be qualified in this case as extremely ordered microshears areas localized on the spectrum of scales and corresponding spacing.

EXPERIMENTAL STUDY

The mechanisms of plastic strain localization in the material subjected to dynamic loading were studied in a split Hopkinson pressure bar using the specimens made of aluminum alloy AMg6, which exhibits the plastic flow instability. The skewed specimens were used to initiate the plastic strain localization at sufficiently high strain rates. It is important that the surface quality, metallurgical effects does not affect on dynamic plastic strain localization on such specimens.

The dissipation-driven temperature fields observed in the specimens subjected to deformation in the Hopkinson pressure bar set-up were investigated by CEDIP Silver 450M high-speed infrared camera (Fig.1), [38,39]. The main characteristics of the camera are as follows: sensitivity not less than 25 mK at 300°K, spectral range 3-5 μm, maximum frame size 320x240 pxl, spatial resolution ("pixel size") ~ 0.2 mm, time resolution ~ 0.25 ms. During deformation, the temperature fields were visualized "in situ". Fig. 1 presents the graph of dependence of temperature on the coordinate at a selected instant of time, the sketch of the specimen, the infrared image of the AMg6 specimen and the scheme of the experiment.

The temperature of the plastic strain localization area does not exceed ~150°C. This has led to the conclusion that thermal softening does not play a decisive role in the localized shear mechanism under these loading conditions.

Initiation of ASB localized areas as spatial zones with ordered microshear ensemble can be proposed as the mechanism of the stored energy drop due to the coherent microshear slips and localized plastic flow with the front propagating as the solitary wave front. Transformation of the self-similar solitary wave solution into the blow-up dissipative structures corresponds to the qualitative change of the free energy metastabilty (stored energy release) and extremely high microshear induced strain rates on the set of scales given by the self-similar solution (5). The relative low temperature given by in-situ infrared framing can be linked to the small sizes of area with blow-up microshear dynamics averaged by the infrared resolution.

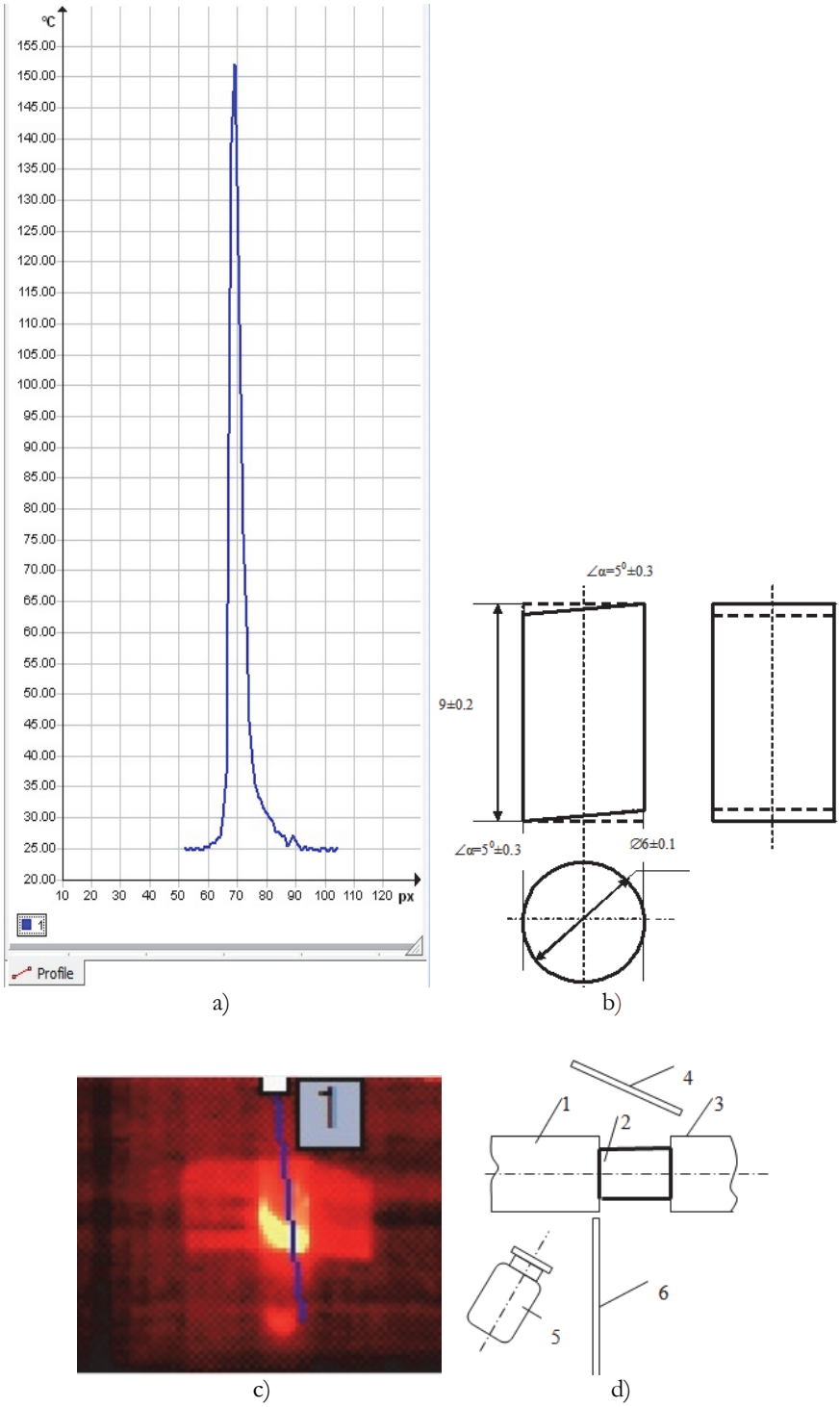

Figure 1: Experimental results for the examined specimen. Plot of temperature variation along the indicated coordinate at the selected instant of time. Maximum temperature is ~ 150°C (a). Skewed specimen made of the AMg6 alloy for studying plastic strain, AMg6 alloy(b). Infrared image of the skewed AMg6 alloy specimen during the experiment (c). Scheme of the experimental procedure: 1 - input bar, 2 - specimen, 3-output bar, 4-mirror, 5-infrared camera, 6- protective screen (d)

Structural studies

Before metallographic studies, the skewed specimens subjected to dynamic tests were pressed into conductive bakelite on a CitoPress-10 machine (Struers) and then polished on a Tegramin-30 machine (Struers). In coarse skinning regimes, a distilled aqueous medium was used as a lubricant, while the lubricant used at the final stages of the finishing process contained highly dispersed silicon oxide particles. The etching was carried out with Keller's reagent for 5-10 seconds at 65-70°C.

The metallographic analysis of skewed specimens was performed before and after dynamic tests on a split Hopkinson pressure bar. The structural study was carried out for longitudinally cut skewed specimens using the light and scanning electron microscopes. Light microscopy was performed with Olympus GX-51 microscope at magnification of 100x-1000x. The metallographic studies were conducted using a FEI PHENOM G2 ProX electron microscope at 15 kV accelerating voltage and 1000x-15000x magnification.

The initial structure of the AMg6 alloy in the test specimens was traditional for this type of alloy and represented a combination of grains of α-phase oriented along the bar axis. A characteristic feature of the initial structure in all investigated specimens is the presence of two types of large elongated grains (crystals): grains, that contain a developed ensemble of smaller grains of about 10-30 microns in size, and grains, in which the developed inner grain substructure is almost completely absent. The diametric dimensions of grains in the initial structure of the examined specimens are close being about 10-20 μm in the ensemble of fine grains and about 120-140 μm in the ensemble of large grains, in which there are no signs of the developed inner grain substructure (Fig. 2, a-c).

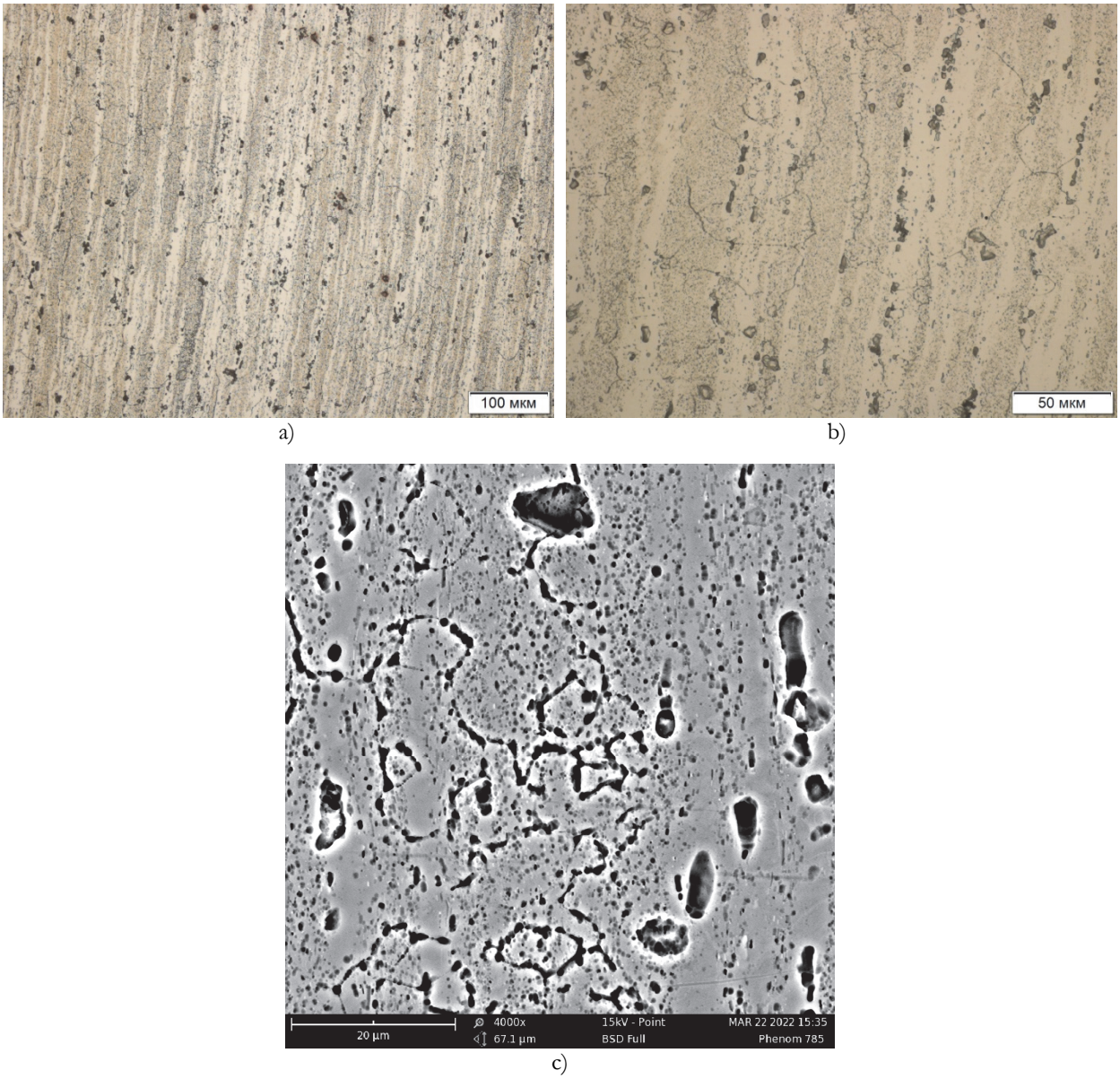

a) b)

c)

Figure 2: Initial structure of the examined specimen (longitudinal section); a - x50; b - x500; and c - x4000; a,b - light microscopy; c - electron microscopy.

Analysis of the specimen structure after testing on the split Hopkinson pressure bar revealed the zone of stress concentration, which triggered the process of structural transformation, accompanied by the formation of a localized shear band structure.

The results of structural analysis of the specimens after testing on the split Hopkinson pressure bar are shown in Fig. 3, a-e. It was found that the processes of plastic deformation with characteristic stretching and bending of both large grains and ensembles of small grains of the initial structure occurred in the central part of the general stress concentration zone. The structural volumes (grains), in which the conditions for plastic deformation were realized, became the sites of formation of structural elements with characteristic features of localized shear bands (Fig. 3, e). In the peripheral region, the observed nucleation of microcracks was also accompanied by the formation of structural elements at their tips with characteristic features of localized shear bands (Fig.3, d). It should also be noted that in the specimens under study the number of structural volumes, in which the processes of structural transformation involved the formation of localized shear bands is rather great. The area with localized shear bands with pronounced orientation collective mode can be associated with DRX areas.

a)

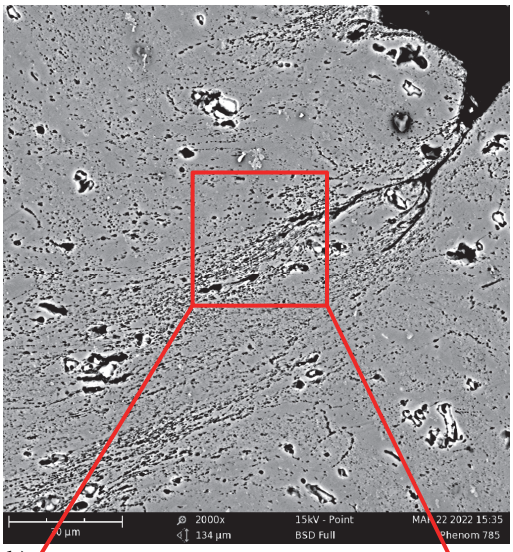

b)

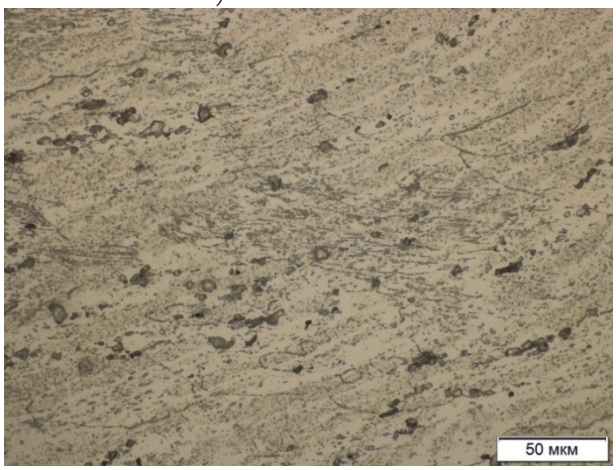

c)

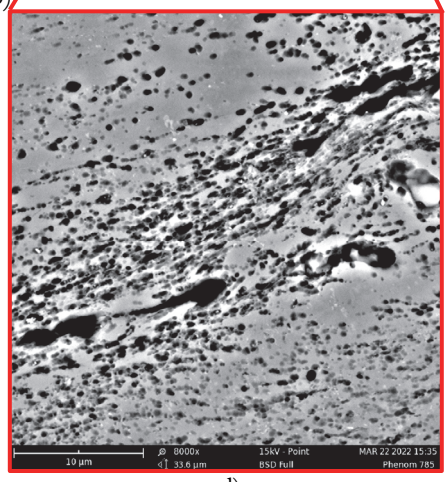

d)

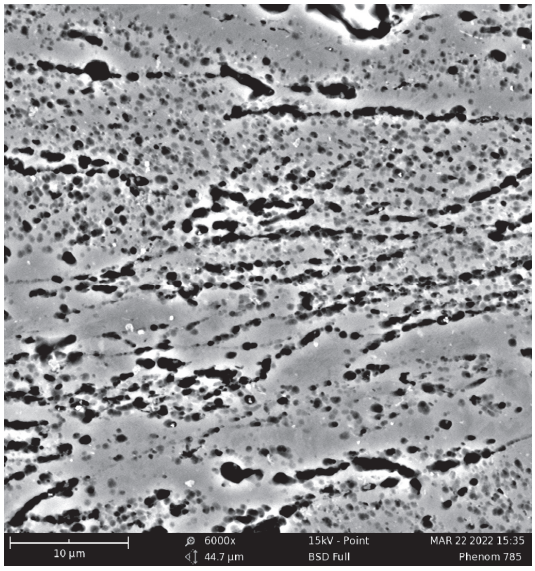

e)

Figure 3: Structure of the examined specimen after tests in the split Hopkinson pressure bar; a, c, e- central part of the stress concentration zone; b, d- peripheral part of the stress concentration zone; a-e - longitudinal section; a - x200; c - x500; e - x6000; b - x2000; d - x8000; a, c - light microscopy; b, d, e - electron microscopy.

Numerical simulation

The modeling of the ASB staging, plastic strain localization and transition to ASB failure was done using the constitutive equations reflecting the role of structural-scaling transitions in microshears ensemble as specific type of criticality in solids with mesodefects in the presence of the free energy metastability and corresponding free energy (or stored energy) release. Two important features of the ASB staging were presented in the constitutive equations as the qualitative new modeling strategy based on the non-linear dynamics of the hidden structural variables (microshear density tensor and structural scaling parameter). There are stored energy metastability decomposition with the generation of collective modes of different complexity (breathers, solitary waves, blow-up dissipative structures) playing the role of collective variables determining spatial-temporal scaling of ASB initiation and interaction, and sudden localized drop of the relaxation time providing the localization of plastic flow. Microshears ensemble dynamics allowed the modeling of geometrical (spatial) critical effects for shear band formation mentioned by Molinari and Clifton [22] and the role of fluctuations to trigger the shear band in contrast to the leading conventional role of temperature inhomogeneity (Wright and Walter [40]).

The loading scheme used for numerical calculation is shown in Fig. 4. The bars of split Hopkinson pressure bar setup were simulated by two cylinders between which the specimen was clamped. The Hopkinson bars are considered to be absolutely solid bodies due to the fact that the modulus of elasticity of AMg6 alloy is nearly three times lower than that of steel, and the yield strength of AMg6 alloy is several times lower than that of steel.

The laws of bar displacement are known from the experiment. The displacements at one bar end are taken to be equal to zero, and the resulting displacements at the other end are specified as the difference in displacements at both ends of the specimen.

The interface between the contacting specimen and the cylinders meet the conditions of ideal contact (frictionless interaction), which corresponds to the loading conditions, since in the experiment, these surfaces were treated with a lubricant. On the other boundaries of the specimen the conditions of free surface are set. Initial conditions specified for all parameters (stress, strain, displacement, microdefects density tensor) are equal to zero.

The processes of elastic-plastic deformation are described by the system of constitutive relations, which is based on the statistical theory of defects described above [41]:

$$\dot{\boldsymbol{\sigma}} = \lambda\left(\dot{\boldsymbol{\varepsilon}}^{e} : \mathrm{E}\right)\mathrm{E} + 2G\dot{\boldsymbol{\varepsilon}}^{e}$$

$$\dot{\boldsymbol{\varepsilon}}^{e} = \dot{\boldsymbol{\varepsilon}} - \dot{\boldsymbol{\varepsilon}}^{p} - \dot{\mathrm{p}}$$

$$\dot{\mathbf{e}}^{p} = \Gamma_{\sigma}\boldsymbol{\sigma} - \Gamma_{p\sigma}\frac{\partial F}{\partial \mathbf{p}}$$

$$\dot{\mathrm{p}} = \Gamma_{p\sigma}\boldsymbol{\sigma} - \Gamma_{p}\frac{\partial F}{\partial \mathrm{p}}$$

where $\dot{\mathbf{e}}$ is the strain rate tensor, $\dot{\mathbf{e}}^{e}$, $\dot{\mathbf{e}}^{p}$, $\dot{\mathrm{p}}$ are its elastic, plastic and defective components, $\boldsymbol{\sigma}$ is the stress tensor, $\boldsymbol{E}$ is the unit tensor, λ = 41 GPa, G = 27 GPa are the Lame elastic constants, Γ_{σ} = 1.85·10-8 $(Pa{\cdot}s)^{-1}$, $\Gamma_{p\sigma}$ = 0.4·10-8 $(Pa{\cdot}s)^{-1}$, $\Gamma_{p\sigma}$ = 0.1·10-8 $(Pa{\cdot}s)^{-1}$ are the kinetic coefficients.

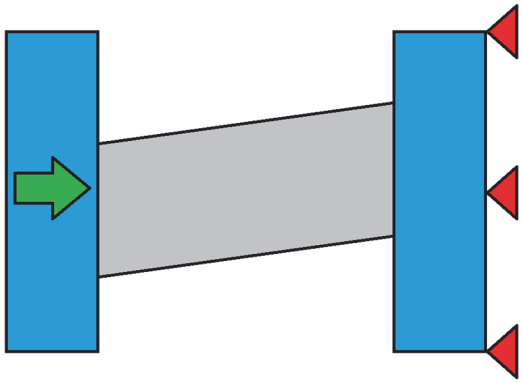

Figure 4: Scheme of specimen loading used in calculations

The problem was solved numerically by the finite element method. A uniform mesh with a characteristic finite element size equal to 1/100 of the specimen height (length) was used to cover the integration domain. It was shown that this element size was sufficient for adequate calculations. The simulation was carried out using the C3D8R finite elements representing hexagonal, 8-node elements with linear approximation.

The numerical algorithm and original numerical code [38] were used for the simulation of the experiment and the results of simulation are shown in Fig.5. The comparison of the temperature fields obtained experimentally with the results of simulations carried out taking into account the kinetics of accumulation of mesodefects gives satisfactory agreement to an accuracy of ~20%.

In the process of high-speed deformation, a structural-kinetic transition occurs in the material in terms of the microshears density parameter in the local region, which is characterized by a rapid increase in the microshears density with a sharp change in the effective relaxation time and, as a result, to a sharp increase of plastic strain rate, stress relaxation and the drop in shear resistance on characteristic lengths of material. A sharp drop in the resistance of solid to shear loads, the appearance of areas of plastic shear instability are due to the pronounced orientation ordering in microshears ensemle. The temperature values in the localization zone obtained in the experiment and as a result of numerical simulation indicate that for the aluminum alloy AMg6 there are no conditions for the implementation of the mechanism of thermoplastic instability under the realized loading conditions.

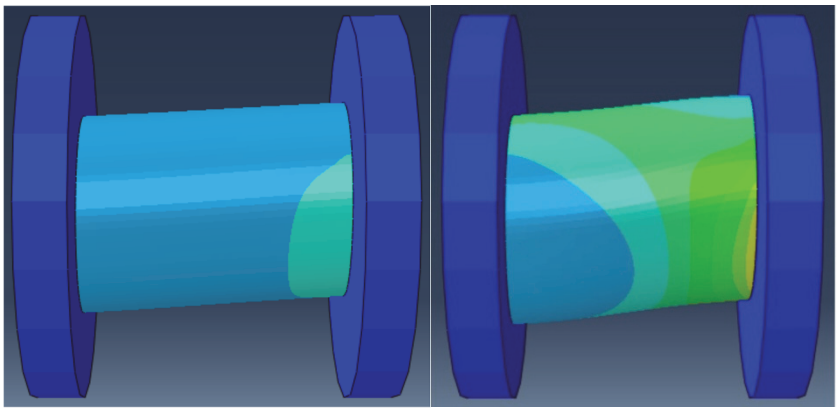

a) b)

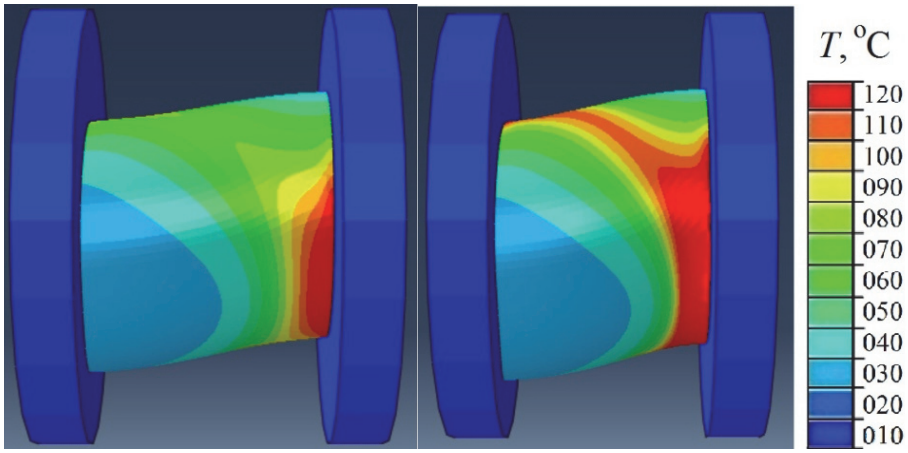

c) d)

Figure 5: Temperature distribution in the examined AMg6 alloy specimen at different moments of time (from left to right and from top to bottom): a- $1 \cdot 10^{-4}$ s, b - $2 \cdot 10^{-4}$ s, c- $3 \cdot 10^{-4}$ s, d - $4 \cdot 10^{-4}$ s

Conclusion

New concept of ASB initiation and ASB induced failure is proposed based on the original results established new type of critical behavior of mesodefects (microshears, microcracks) ensemble. The mesodefects ensemble evolution follows to the free energy release reflecting the metastability of the "stored energy" in the terms of two "order parameters": the mesodefects induced strain and structural scaling parameter providing the accounting of initial and current structural susceptibility of solid to the defects growth.

The explanation of ASB staging scenario is given using the self-similar solutions for mesodefects evolution equation reflecting the consequent transformation of microshears ensemble kinetics from the solitary wave to blow-up spatial-temporal collective modes. Consequent dynamics given by three types of self-similar solutions (breathers, solitary waves and blow-up dissipative structures) corresponds to three stages of ASB failure. The first is characterized by the strain pattern formation at the first critical point of structural-scaling parameter and triggering the breathers dynamics, which leads to the spatially distributed strain pattern with pronounced orientation mode in microshears ensemble. The spatial scaling of this pattern provides structural and strain heterogeneity shifting the free energy release into the metastabity area in some part of the material and initiation of solitary wave microshears modes. Evolution of these modes describes the transition to the ASB second stage with the formation of solitary wave front with the length, velocity and amplitude according to "metastability decomposition" kinetics. The solitary wave dynamics determines the multiscale momentum diffusion due to the ASB front propagation with pronounced multiscale microshears ordering in the ASB process area.

Numerous initiation of the solitary wave strain localization modes leads to qualitative new pattern formation with scaling properties initiating the path of the second critical point and transforming the solitary wave modes into the blow-up modes and ASB failure on the set of "fundamental lengths".

It allows the explanation of the role of numerous correlated shearing discussed by Grady [3] as mechanism of the steady shock compression front universality. This behavior has been observed in the steady-wave shock compression of a number of solids [37].

The infrared image of temperature field during dynamic loading of the AMg6 alloy, the structural studies by electron microscopy and the results of numerical simulation of microshear induced damage kinetics [38, 39] allow us to hypothesize that the mechanisms of plastic strain localization for the AMg6 alloy at high strain loading can be associated with the shear band self-organization with pronounced signs of critical phenomena in defects ensemble.

Acknowledgements

This research was supported by the Russian Science Foundation (project 21-79-30041), https://rscf.ru/en/project/21-79-30041/

REFERENCES

[1] Wright, T.W. (2002). The Physics and Mathematics of Adiabatic Shear Bands. Cambridge University Press, Cambridge, England, Cambridge University Press.

[2] Batra, R.C. (1987). The initiation and growth of, and the interaction among, adiabatic shear bands in simple and dipolar materials, Int. J. Plasticity, 3, pp. 75-89.

[3] Grady, D.E., Kipp M. E. (1987). The growth of unstable thermoplastic shear with application to steady-wave shock compression in solids, J. Mech. Phys. Solids, 35(1), pp.95–119. DOI: 10.1016/0022-5096(87)90030-5

[4] Zener, C., Hollomon, J. (1944). Effect of strain rate upon plastic flow of steel, J. Appl. Phys., 14, pp.22–32.

[5] Wright, T.W. (1987). Some aspects of adiabatic shear bands, In: Metastability and Incompletely Posed Problems, Berlin, Springer-Verlag, pp. 353-372.

[6] Armstrong, R., Batra, R.C., Meyers, M., Wright, T.W., editors. (1994). Shear instabilities and viscoplasticity theories, Mech. Mater., 17, pp. 83–328.

[7] Marchand A., Duffy J. (1988). An experimental study of the formation process of adiabatic shear bands in a structural steel, J. Mech. Phys. Solids, 36(3), pp. 251-283. DOI: 10.1016/0022-5096(88)90012-9

[8] Duffy, F. (1991). Experimental study of shear band formation through temperature measurements and high speed photography, J. Phys. IV, 1(C3), pp. 645-652.

[9] Batra, R. C., Adulla, C., Wright, T. W. (1996). Effect of defect shape and size on the initiation of adiabatic shear bands, Acta Mech., 116, pp. 239-243.

[10] Molinari, A. (1997). Collective behavior and spacing of adiabatic shear bands, J. Mech. Phys Solids, 45, pp. 1551–1575.

[11] Backman, M. E., Finnegan, S. A. (1973). The propagation of adiabatic shear, In: Metallurgical effects at high strain rates, New York, Plenum Press, pp. 531 -543.

[12] Wright, T.W. (1974). Toward a defect invariant basis for susceptibility to adiabatic shear bands, Mech. Materials, 17, pp. 215-222.

[13] Wei, Z.G., Batra, R.C. (2002). Dependence of instability strain upon damage in thermoviscoplastic materials, Arch. Mech., 54, pp. 691–707.

[14] Batra, R.C., Wei, Z.G. (2006). Shear band spacing in thermoviscoplastic materials, Int. J. Impact Eng., 32, pp. 947–967.

[15] Clifton, R.J., Duffy, J., Hartley, K.A., Shawki, T.G. On critical conditions for shear band formation at high strain rates, Scripta Metall., 18(5), pp.443–448. DOI: 10.1016/0036-9748(84)90418-6.

[16] Bai, Y.L. A Criterion for Thermoplastic Shear instability, In: Shock Waves and High Strain Rate Phenomenon in Metals, New York, Plenum Press, pp. 277- 283.

[17] Wright, T.W. (1994). Toward a defect invariant basis for susceptibility to adiabatic shear bands Mechanics of Materials, 17(2-3), pp. 215-222. DOI: 10.1016/0167-6636(94)90061-2.

[18] Wright, T.W.(1992). Shear band susceptibility: Work hardening materials, Int. J. Plast., 8(5), pp. 583-602. DOI: 10.1016/0749-6419(92)90032-8.

[19] Batra, R.C., Love, B.M. (2006). Consideration of microstructural effects in the analysis of adiabatic shear bands in a tungsten heavy alloy , Int. J. Plasticity, 22, pp.1858–1878.

[20] Fressengeas, C , and Molinari, A., (1987). Instability and Localization of Plastic Flow in Shear at High Strain Rates, Mech. Phys. Solids, 35, pp. 185-211.

[21] Molinari A. (1997). Collective behavior and spacing of adiabatic shear bands, J Mech Phys Solids,45, pp.1551–1575.

[22] Molinari A. and Clifton R. J. (1987). Analytical Characterization of Shear Localization in Thermoviscoplastic Materials, J. Appl. Mech., 54, pp. 806–812.

[23] Wright, T.W. (1990). Adiabatic shear bands, Appl. Mech. Rev., 43(5S), pp. 196-200. DOI: 10.1115/1.3120804.

[24] Rittel, D., Landau, P., and Venkert, A. (2008). Dynamic recrystallization as a potential cause for adiabatic shear failure, Phys. Rev. Lett., 101, pp. 165501-1- 165501-4.

[25] Rittel, D. (2009). A different viewpoint on adiabatic shear localization, J. Phys. D: Appl. Phys., 42, pp.214009-1 – 214009-6. DOI: 10.1088/0022-3727/42/21/214009.

[26] Xu, Y.B. and Bai, Y.L. (2007). Shear localization, microstructure evolution and fracture under high-strain rate, Adv. Mech. 37, pp. 496 – 516.

[27] Murr, L.E. and Esquivel, E.V. (2004). Observations of common microstructural issues associated with dynamic deformation phenomena: twins, microbands, grain size effects, shear bands, and dynamic recrystallization, J. Mater. Sci., 39, pp.1153 – 1168.

[28] Martinez, F., Murr L.E., Ramirez A., Lopez M.I., and Gaytan S.M. (2007). Dynamic deformation and adiabatic shear microstructures associated with ballistic plug formation and fracture in Ti–6Al–4V targets, Mater. Sci. Eng.:A, 454–455, pp. 581 – 589. DOI: 10.1016/j.msea.2006.11.097.
[29] Perez-Prado, M.T., Hines, J.A. , and Vecchio K.S. (2001). Microstructural evolution in adiabatic shear bands in Ta and Ta–W alloys, Acta Mater., 49, pp. 2905 - 2917. DOI: 10.1016/S1359-6454(01)00215-4.
[30] Nesterenko V.F., Meyers M.A. and Wright T.W. (1998). Self-organization in the initiation of adiabatic shear bands, Acta Mater., 46(1), pp. 327-340. DOI: 10.1016/S1359-6454(97)00151-1.
[31] Grady, D.E. (1994). Dissipation in adiabatic shear bands, Mech. Mater., 17, pp.289-293. DOI: 10.1016/0167-6636(94)90066-3.
[32] Grady, D.E. (1992). Properties of an adiabatic shear-band process zone, J. Mech. Phys. Solids, 40(6), pp.1197-1215 DOI: 10.1016/0022-5096(92)90012-Q.
[33] Naimark, O.B. (2004). Defect induced transitions as mechanisms of plasticity and failure in multifield continua, In: Advances in Multifield Theories of Continua with Substructure, Boston, Birkhäuser, pp. 75–114. DOI: 10.1007/978-0-8176-8158-6_4
[34] Naimark, O.B. (2003). Collective properties of defects ensemble and some nonlinear problems of plasticity and fracture, Physical Mesomechanics, 6(4), pp.39–63
[35] Kurdyumov, S.P. (1988). Evolution and self-organization laws of complex systems, Int. J. Mod. Phys., (1988). 1(4), pp. 299 – 327. DOI: 10.1142/S0129183190000177.
[36] Naimark, O.B. (2016). Energy release rate and criticality of multiscale defects kinetics, Int. J. Fracture, 202, pp. 271–279. DOI: 10.1007/s10704-016-0161-3.
[37] Swegle J.W. and Grady D.E. (1985). Shock viscosity and the prediction of shock wave rise times , J.Appl.Phys., 58 (2), pp. 692-701.
[38] Bilalov D.A., Sokovikov M.A., Chudinov V.V., Oborin V.A., Bayandin Yu.V., Terekhina A.I., Naimark O.B. (2018). Numerical simulation and experimental study of plastic strain localization under the dynamic loading of specimens in conditions close to a pure shear, J. Appl. Mech. Tech. Ph., 59(7), pp. 1179–1188. DOI: 10.1134/S0021894418070027.
[39] Sokovikov M.A., Chudinov V.V., Oborin V.A., Uvarov S.V., Naimark O.B. (2020). Study of localized shear fracture mechanisms of alloys under dynamic loading, J. Appl. Mech. Tech. Ph., 61(7), pp. 1182 – 1193. DOI: 10.1134/S0021894420070147.
[40] Wright, T.W., Walter, J.W. (1987). On stress collapse in adiabatic shear bands, J. Mech. Phys. Solid., 35, pp. 701-720. DOI: 10.1016/0022-5096(87)90051-2 .
[41] Bayandin, Y., Saveleva, N., Naimark, O. (2019) Steady plastic wave fronts and scale universality of strain localization in metals and ceramics, Frattura ed Integrita Strutturale, 13 (49), pp. 243-256. DOI: 10.3221/IGF-ESIS.49.24.